Spin Dependence of η Meson Production in Proton-Proton Collisions Close to Threshold

P. Adlarson,[1,*] W. Augustyniak,[2] W. Bardan,[3] M. Bashkanov,[4] S. D. Bass,[3] F. S. Bergmann,[5] M. Berłowski,[6] A. Bondar,[7,8] M. Büscher,[9,†] H. Calén,[1] I. Ciepał,[10] H. Clement,[11,12] E. Czerwiński,[3] K. Demmich,[5] R. Engels,[9] A. Erven,[13] W. Erven,[13] W. Eyrich,[14] P. Fedorets,[9,15] K. Föhl,[16] K. Fransson,[1] F. Goldenbaum,[9] A. Goswami,[17,9] K. Grigoryev,[9,18] C.-O. Gullström,[1] L. Heijkenskjöld,[1,*] V. Hejny,[9] N. Hüsken,[5] L. Jarczyk,[3] T. Johansson,[1] B. Kamys,[3] G. Kemmerling,[13,‡] G. Khatri,[3,§] A. Khoukaz,[5] O. Khreptak,[3] D. A. Kirillov,[19] S. Kistryn,[3] H. Kleines,[13,‡] B. Kłos,[20] W. Krzemień,[3] P. Kulessa,[10] A. Kupść,[1,6] A. Kuzmin,[7,8] K. Lalwani,[21] D. Lersch,[9] B. Lorentz,[9] A. Magiera,[3] R. Maier,[9,22] P. Marciniewski,[1] B. Mariański,[2] H.-P. Morsch,[2] P. Moskal,[3] H. Ohm,[9] W. Parol,[10] E. Perez del Rio,[11,12,‖] N. M. Piskunov,[19] D. Prasuhn,[9] D. Pszczel,[1,6] K. Pysz,[10] A. Pyszniak,[1,3] J. Ritman,[9,22,23] A. Roy,[17] Z. Rudy,[3] O. Rundel,[3] S. Sawant,[24] S. Schadmand,[9] I. Schätti-Ozerianska,[3] T. Sefzick,[9] V. Serdyuk,[9] B. Shwartz,[7,8] K. Sitterberg,[5] T. Skorodko,[11,12,25] M. Skurzok,[3] J. Smyrski,[3] V. Sopov,[15] R. Stassen,[9] J. Stepaniak,[6] E. Stephan,[20] G. Sterzenbach,[9] H. Stockhorst,[9] H. Ströher,[9,22] A. Szczurek,[10] A. Trzciński,[2] M. Wolke,[1] A. Wrońska,[3] P. Wüstner,[13] A. Yamamoto,[26] J. Zabierowski,[27] M. J. Zieliński,[3] J. Złomańczuk,[1] P. Żuprański,[2] and M. Żurek[9]

(WASA-at-COSY Collaboration)

[1]*Division of Nuclear Physics, Department of Physics and Astronomy, Uppsala University, Box 516, 75120 Uppsala, Sweden*
[2]*Department of Nuclear Physics, National Centre for Nuclear Research, ul. Hoza 69, 00-681Warsaw, Poland*
[3]*Institute of Physics, Jagiellonian University, prof. Stanisława Łojasiewicza 11, 30-348 Kraków, Poland*
[4]*School of Physics and Astronomy, University of Edinburgh, James Clerk Maxwell Building, Peter Guthrie Tait Road, Edinburgh EH9 3FD, United Kingdom*
[5]*Institut für Kernphysik, Westfälische Wilhelms-Universität Münster, Wilhelm-Klemm-Straße 9, 48149 Münster, Germany*
[6]*High Energy Physics Department, National Centre for Nuclear Research, ul. Hoza 69, 00-681 Warsaw, Poland*
[7]*Budker Institute of Nuclear Physics of SB RAS, 11 akademika Lavrentieva prospect, Novosibirsk 630090, Russia*
[8]*Novosibirsk State University, 2 Pirogova Str., Novosibirsk 630090, Russia*
[9]*Institut für Kernphysik, Forschungszentrum Jülich, 52425 Jülich, Germany*
[10]*The Henryk Niewodniczański Institute of Nuclear Physics, Polish Academy of Sciences, 152 Radzikowskiego St, 31-342 Kraków, Poland*
[11]*Physikalisches Institut, Eberhard-Karls-Universität Tübingen, Auf der Morgenstelle 14, 72076 Tübingen, Germany*
[12]*Kepler Center für Astro-und Teilchenphysik, Physikalisches Institut der Universität Tübingen, Auf der Morgenstelle 14, 72076 Tübingen, Germany*
[13]*ZentralInstitut für Engineering, Elektronik und Analytik, Forschungszentrum Jülich 52425 Jülich, Germany*
[14]*Physikalisches Institut, Friedrich-Alexander-Universität Erlangen-Nürnberg, Erwin-Rommel-Str. 1, 91058 Erlangen, Germany*
[15]*Institute for Theoretical and Experimental Physics, State Scientific Center of the Russian Federation, Bolshaya Cheremushkinskaya 25, 117218 Moscow, Russia*
[16]*II. Physikalisches Institut, Justus-Liebig-Universität Gießen, Heinrich-Buff-Ring 16, 35392 Giessen, Germany*
[17]*Department of Physics, Indian Institute of Technology Indore, Khandwa Road, Simrol, Indore 453552, Madhya Pradesh, India*
[18]*High Energy Physics Division, Petersburg Nuclear Physics Institute, Orlova Rosha 2, Gatchina, Leningrad district 188300, Russia*
[19]*Veksler and Baldin Laboratory of High Energiy Physics, Joint Institute for Nuclear Physics, 6 Joliot-Curie, Dubna 141980, Russia*
[20]*August Chełkowski Institute of Physics, University of Silesia, Uniwersytecka 4, 40-007 Katowice, Poland*
[21]*Department of Physics, Malaviya National Institute of Technology Jaipur, JLN Marg Jaipur 302017, Rajasthan, India*
[22]*JARA-FAME, Jülich Aachen Research Alliance, Forschungszentrum Jülich, 52425 Jülich, and RWTH Aachen, 52056 Aachen, Germany*
[23]*Institut für Experimentalphysik I, Ruhr-Universität Bochum, Universitätsstr. 150, 44780 Bochum, Germany*
[24]*Department of Physics, Indian Institute of Technology Bombay, Powai, Mumbai 400076, Maharashtra, India*
[25]*Department of Physics, Tomsk State University, 36 Lenina Avenue, Tomsk 634050, Russia*
[26]*High Energy Accelerator Research Organisation KEK, Tsukuba, Ibaraki 305-0801, Japan*
[27]*Department of Astrophysics, National Centre for Nuclear Research, 90-950 Łódź, Poland*

(Received 7 September 2017; revised manuscript received 3 November 2017; published 8 January 2018)

Taking advantage of the high acceptance and axial symmetry of the WASA-at-COSY detector, and the high polarization degree of the proton beam of COSY, the reaction $\vec{p}p \to pp\eta$ has been measured close to threshold to explore the analyzing power A_y. The angular distribution of A_y is determined with the precision

improved by more than 1 order of magnitude with respect to previous results, allowing a first accurate comparison with theoretical predictions. The determined analyzing power is consistent with zero for an excess energy of $Q = 15$ MeV, signaling s-wave production with no evidence for higher partial waves. At $Q = 72$ MeV the data reveal strong interference of Ps and Pp partial waves and cancellation of $(Pp)^2$ and $Ss^* Sd$ contributions. These results rule out the presently available theoretical predictions for the production mechanism of the η meson.

DOI: 10.1103/PhysRevLett.120.022002

In recent decades, hadron physics has been rich in discoveries in the low-energy region where the interaction between hadrons is a manifestation of the strong force between their components [1–5]. However, there are still many open questions involving the nonperturbative dynamics and details of hadron production processes. Spin observables offer an essential tool to yield new insight into this physics. In this Letter, we focus on η meson production in low-energy proton-proton collisions with a polarized proton beam. We report the first precise measurements of the analyzing power for the $\vec{p}p \to pp\eta$ reaction at two energies close to threshold. These measurements yield new powerful constraints on models of the η production.

The presented results are based on about 200 times larger statistics and drastically reduced systematic uncertainties with respect to the previous experiments [6–8]. The main improvement of systematics is due to (i) axial symmetry and full acceptance of the WASA-at-COSY detector (more than 20 times larger than for the COSY-11 experiment [9]), (ii) no magnetic field in the detector; in addition, the systematics was controlled by the measurements (iii) for two spin orientations and (iv) for two different decay channels of the η meson.

Previous studies by the CELSIUS [10–13], COSY [14–18], and SATURNE [19–21] experiments of the total and differential cross sections for η meson production in pp and pn collisions revealed that the η meson is predominantly produced via the excitation of one of the nucleons to the S_{11} current via exchange of virtual mesons with the subsequent decay into the proton-η pair. This conclusion was obtained from the observation of a large η production cross section relative to the η' meson production and the isotropic angular distribution of the η mesons in the center-of-mass (c.m.) system. Measurements of the total cross section for η production in different isospin channels [13,18] revealed a strong contribution from isovector exchanges that is additive in proton-neutron collisions and that (partially) cancels in proton-proton collisions, bringing more constraints on theoretical models. While much progress has been achieved, the mechanism for the excitation of the colliding proton to a resonance state still remains very much incomplete, with a host of models each with different weighting of exchanges proposed to explain the dynamics.

Here, we use spin as a tool to gain further insights. The experiment involves a polarized proton beam with incident momentum in the z direction and transversely polarized in the y direction, colliding with an unpolarized fixed proton target. The analyzing power is a sensitive extra constraint on the details of the η production mechanism.

The η meson production process proceeds through exchange of a complete set of virtual meson hadronic states, which, in models, is usually truncated to single-virtual-meson exchange. Theoretical models have been proposed involving π, η, ρ, ω, and σ (correlated two-pion) exchanges [22–27] and excited nucleon resonances, primarily the $S_{11}(1535)$ plus small contributions from the $D_{13}(1520)$ and $P_{11}(1440)$ [23,24]. OZI-violating gluonic excitations might also couple to the flavor-singlet part of the η meson in short-distance proton-proton interactions [28]. These exchanges induce very different spin dependence in the production process. Polarized beams and measurement of the analyzing power can therefore put powerful new constraints on theoretical understanding of the η production process. For example, ρ exchange and π exchange models predict a near-threshold analyzing power with different signs [22,24]. Isotropic (pure s-wave) production would give zero analyzing power.

The measurements of the $\vec{p}p \to pp\eta$ reaction were conducted by means of the large acceptance close to 4π and an axially symmetric WASA-at-COSY spectrometer, operating as an internal fixed-target facility at the Cooler Synchrotron COSY [29]. The vertically polarized proton beam was circulating through the vertical stream of the hydrogen pellets, leading to the $\vec{p}p \to pp\eta$ reaction in the center of the WASA-at-COSY detector. The measurements were performed for the beam momentum values of 2026 MeV/c and 2188 MeV/c, corresponding to excess energies in the c.m. system of $Q = 15$ MeV and 72 MeV, respectively. The orientation of the proton beam polarization was flipped for each accelerator cycle, which lasted 90 s.

The charged hadronic ejectiles were registered by means of forward scintillator hodoscopes, and the straw tube trackers were identified using the energy deposited in the subsequent scintillator layers. The η mesons were detected by the electromagnetic calorimeter and the plastic scintillator barrel. The production of the η meson via the $\vec{p}p \to pp\eta$ reaction was identified using missing and invariant mass techniques. In total, more than 400 000 η meson events were identified and used for the determination of the analyzing power.

The center of the interaction region where the polarized proton beam collided with the pellet target was monitored

with a precision of about 0.5 mm by the concurrent measurement of elastically scattered protons. The superconducting solenoid was switched off in order to minimize losses of the spin polarization. Only neutral decay products of the η meson were reconstructed. In particular, the $\eta \to \gamma\gamma$ and $\eta \to 3\pi^0 \to 6\gamma$ decay channels with the highest branching ratios (altogether over 71% [30]) were used in the presented analysis. A detailed description of the WASA-at-COSY experiment, as well as methods and results of the monitoring of the interaction region, was given in the dedicated articles [31–34].

The analyzing power $A_y(\theta_\eta)$ for the given polar angle θ_η of the emission of the η meson in the c.m. system was determined from the asymmetry of the efficiency-corrected η meson production yields N_η,

$$\text{Asymmetry}(\theta_\eta, \phi_\eta) \equiv \frac{N_\eta(\theta_\eta, \phi_\eta) - N_\eta(\theta_\eta, \phi_\eta + \pi)}{N_\eta(\theta_\eta, \phi_\eta) + N_\eta(\theta_\eta, \phi_\eta + \pi)} \quad (1)$$

extracted as a function of the azimuthal angle ϕ_η,

$$\text{Asymmetry}(\theta_\eta, \phi_\eta) = PA_y(\theta_\eta)\cos(\phi_\eta), \quad (2)$$

where P denotes the degree of the spin polarization of the proton beam. In the presented analysis, the Madison convention [35] was applied to fix the sign of the asymmetry.

The yields of the η meson production N_η were determined based on the missing-mass spectra, independently for each (θ_η, ϕ_η) angular range. Examples of spectra for a chosen angular range are presented in Fig. 1. The spectra show only a small range of masses close to the kinematical limit, where a clear signal from the production of the η meson is seen on top of the multipion production background. It is important to stress that the missing mass spectra for the $pp \to pp2\gamma$ reaction channel shown in Fig. 1 (left panel) include a background that is much larger when compared to the nearly negligible background observed for the $pp \to pp6\gamma$ reaction shown in Fig. 1 (right panel) [36]. The contribution of the background was estimated by a fit to the experimental spectra of the shapes of missing mass distributions simulated for the production of the π^0, $2\pi^0$, and $3\pi^0$. The data simulated for the multipion production reaction included the response of the detector system and were analyzed using the same procedures as used for the analysis of the experimental events. Next, after subtraction of the background, the number of the registered η mesons was determined and corrected for the efficiency. The efficiency for the reconstruction of the $pp \to pp\eta$ reaction was established for each angular bin $(\theta_\eta,\ \phi_\eta)$ separately, based on the Monte Carlo simulation performed taking into account the geometrical acceptance of the WASA-at-COSY detector, as well as the experimental detection efficiencies and energy and angular resolutions. The angular bin size (18 degrees for θ_η and 30 degrees for ϕ_η) was chosen based on the statistical significance of events in each bin.

Figure 2 gives an illustration of our results for asymmetries for the $\vec{p}p \to pp\eta$ reaction yield as a function of the azimuthal angle ϕ_η of the η meson momentum vector in the c.m. system. A fit of Eq. (2) to the angular dependence of the asymmetry enables one to determine the product PA_y, which divided by the polarization P, gives the value of the analyzing power A_y.

The polarization P was determined for each spin orientation and each excess energy separately, by the simultaneous measurement of asymmetries for the elastically scattered protons for which the analyzing power is known [37,38]. The method of the polarization analysis is described in detail in Refs. [36,39,40], and the resulting

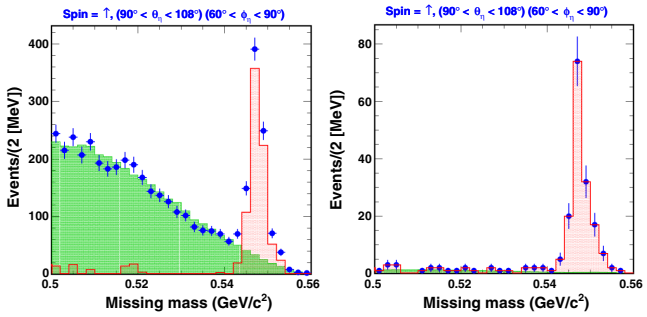

FIG. 1. Examples of missing-mass distributions obtained for the excess energy $Q = 15$ MeV: (left panel) $\vec{p}p \to pp2\gamma$ and (right panel) $\vec{p}p \to pp3\pi^0 \to pp6\gamma$ reactions. The legends above the figures indicate the spin orientation and the angular intervals. Experimental data are denoted by solid blue circles. Vertical bars indicate the statistical uncertainty. The shaded green area denotes the simulated contribution from multipion production background. The shaded red histograms correspond to the η events obtained by subtracting the multipion background.

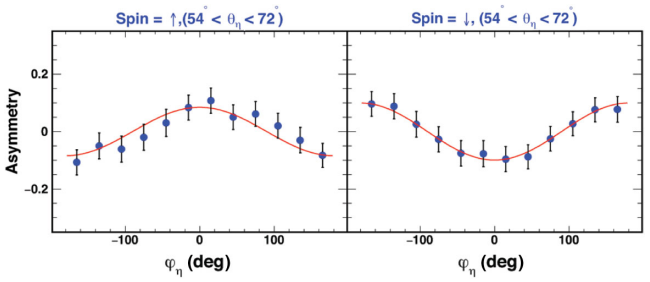

FIG. 2. Example of asymmetry distributions as a function of the ϕ_η angle for a chosen θ_η angular bin, for an excess energy $Q = 72$ MeV and the $\vec{p}p \to pp\eta \to 6\gamma$ reaction. Filled blue points denote extracted asymmetry values with the statistical uncertainty, while the red curves indicates the fit of Eq. (2) to the experimental points. The legend above the figures indicates spin orientation and the angular intervals. The asymmetry for spin-up orientation is about 0.8 times smaller than the asymmetry for spin-down, which is consistent with the ratio of the polarization values determined for different spin orientations (Table I).

TABLE I. The average polarization degree.

p_{beam} (MeV/c)	Spin mode	Polarization
2026	up (↑)	0.793 ± 0.010
	down (↓)	-0.577 ± 0.007
2188	up (↑)	0.537 ± 0.009
	down (↓)	-0.635 ± 0.011

values, together with corresponding statistical uncertainties, are listed in Table I. The systematic uncertainty of the polarization determination amounts to about 0.01 and, as it is shown in detail in Ref. [41], it is predominantly due to the uncertainty of the reconstruction of the position of the interaction region. It is also important to stress that the spin polarization was stable during the whole run [36,39,40] and that, as expected, the analysis of the data taken with the unpolarized beam resulted in the asymmetry equal to zero within the uncertainties [36,40].

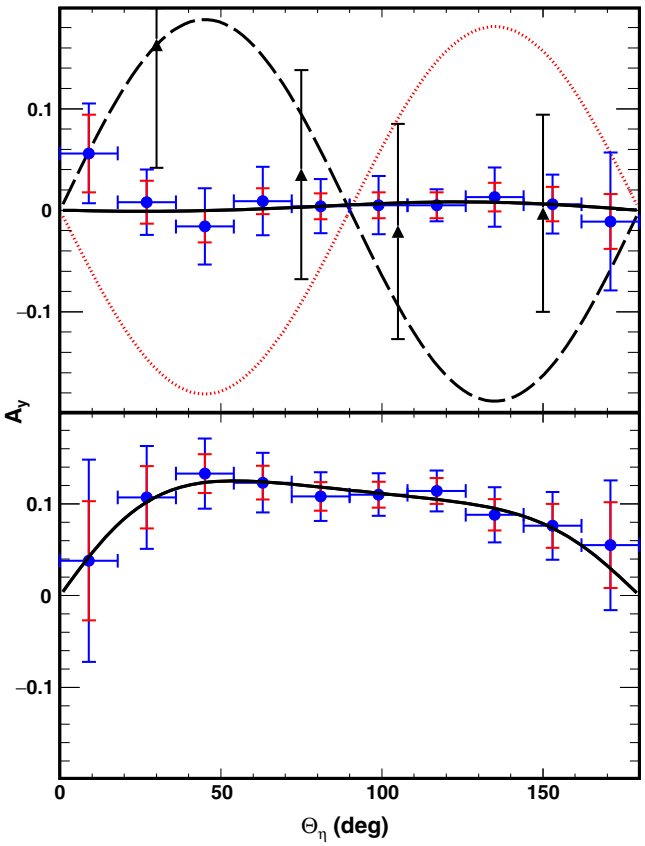

FIG. 3. (Upper panel) Analyzing power for the $\vec{p}p \to pp\eta$ reaction as a function of θ_η for $Q = 15$ MeV. The full circles represent the results obtained in this work, while the triangles are the values of the analyzing powers measured by the COSY-11 Collaboration for $Q = 10$ MeV [7]. Horizontal error bars indicate the angular range. The vertical bars show total uncertainties with statistical and systematic errors separated by dashes. The superimposed dotted line denotes the predictions based on the pseudoscalar-meson-exchange model [24], whereas the dashed line represents the vector exchange model [22]. The result of the fit of Eq. (4) to the data is presented by the solid line. (Bottom panel) Analyzing power for the $\vec{p}p \to pp\eta$ reaction for the $Q = 72$ MeV.

Calculations of the analyzing power A_y were conducted separately for spin-up and spin-down orientations, and for each spin mode, the A_y was determined separately for two decay channels: $\eta \to 2\gamma$ and $\eta \to 6\gamma$. Moreover, for all the above cases, the number of events N_η corresponding to the $\vec{p}p \to pp\eta$ reactions has been determined for each angular bin (θ_η, ϕ_η) separately. This enabled us to control systematic uncertainties that may occur because of the misalignment of the detector and because of the methods of event reconstruction. The final results obtained by averaging values determined for both spin orientations and both decay channels are given in Table II and are presented in Fig. 3. Because of the axial symmetry of the detector, any unknown detector asymmetries and unknown efficiencies should cancel when averaging results obtained for two opposite spin orientations. However, the differences in these results were taken into account in the estimation of the systematic errors. The systematic uncertainties listed in the table have been estimated by calculating changes in the values of A_y to the variation of the parameters used in the analysis. After changing a tested parameter, the full analysis chain was repeated and new A_y values were determined. In particular, the following contributions to the systematic error were taken into account [36]: (i) selection criteria used in the particle identification, (ii) range in the missing mass spectra used for counting the number of produced η mesons, (iii) differences between A_y values obtained for different decay channels, (iv) uncertainty of the values of polarization, and (v) differences between A_y values obtained for spin-up and spin-down measurements. The largest impact on the systematic error comes from the A_y measurement combining different decay channels of the η meson.

Integrating over the proton degrees of freedom results in the analyzing power $A_y(\theta_\eta)$, which, in a partial-wave decomposition, may be expressed as follows:

TABLE II. Analyzing power A_y with statistical and systematic uncertainties determined for the $\vec{p}p \to pp\eta$ reaction at excess energies of $Q = 15$ MeV and $Q = 72$ MeV.

θ_η (deg)	$A_y(\theta_\eta)$ for $Q = 15$ MeV	$A_y(\theta_\eta)$ for $Q = 72$ MeV
0–18	$0.056 \pm 0.038 \pm 0.011$	$0.038 \pm 0.065 \pm 0.045$
18–36	$0.008 \pm 0.021 \pm 0.011$	$0.107 \pm 0.034 \pm 0.022$
36–54	$-0.016 \pm 0.016 \pm 0.022$	$0.133 \pm 0.021 \pm 0.017$
54–72	$0.009 \pm 0.013 \pm 0.021$	$0.123 \pm 0.018 \pm 0.014$
72–90	$0.004 \pm 0.013 \pm 0.014$	$0.108 \pm 0.016 \pm 0.011$
90–108	$0.005 \pm 0.013 \pm 0.046$	$0.110 \pm 0.014 \pm 0.009$
108–126	$0.005 \pm 0.013 \pm 0.003$	$0.114 \pm 0.014 \pm 0.008$
126–144	$0.013 \pm 0.014 \pm 0.015$	$0.088 \pm 0.017 \pm 0.013$
144–162	$0.006 \pm 0.017 \pm 0.012$	$0.076 \pm 0.024 \pm 0.013$
162–180	$-0.011 \pm 0.027 \pm 0.041$	$0.055 \pm 0.047 \pm 0.024$

$$A_y(\theta_\eta)\frac{d\sigma}{d\Omega_\eta} = 2\pi[G_1^{y0}\sin\theta_\eta + (H_1^{y0} + I^{y0})\sin 2\theta_\eta]. \quad (3)$$

Here, the form factors G_1^{y0}, H_1^{y0}, and I^{y0} are defined by Winter *et al.* [6], who generalize the analysis of spin dependence of π^0 production with polarized proton beams to η production [42]. The superscript $y0$ indicates beam polarization along the y axis and an unpolarized target.

We apply the usual spectroscopic notation to describe the $pp \to pp\eta$ process, viz. ${}^{2S^i+1}L^i_{J^i} \to {}^{2S+1}L_J$, l. Here, the relative orbital angular momentum of the two outgoing protons in their rest frame is denoted by capital letters $L_p = S, P, D, \ldots$, and the one of the η meson in the c.m. system by the lowercase letters $l_q = s, p, d, \ldots$ With this notation, the individual terms G_1^{y0}, H_1^{y0}, and I^{y0} correspond to (Ps^*Pp), $(Pp)^2$, and (Ss^*Sd) interference, respectively. The Pauli principle means that even and odd partial waves of the protons in the final state cannot interfere with each other. In total, with polarized beams there are one Ss, two Ps, nine Pp, and two Sd final-state production amplitudes [42]. For example, the Ss amplitude corresponds to the process ${}^3P_0 \to {}^1S_0$, s. The $(Pp)^2$ and Ss^*Sd interference amplitudes always appear together in the analyzing power and angular distribution [42].

Following Eq. (3), we fit the data as

$$A_y(\theta_\eta)\frac{d\sigma}{d\Omega_\eta} = C_1\sin\theta_\eta + C_2\cos\theta_\eta\sin\theta_\eta, \quad (4)$$

where C_1 and C_2 are treated as free parameters. For $Q = 15$ MeV, the angular distribution of the cross section $(d\sigma/d\Omega_\eta)$ is assumed to be constant as determined by the COSY-11 [16] and COSY-TOF [15] experiments. For the fit at $Q = 72$ MeV, the $(d\sigma/d\Omega_\eta)$ determined by the WASA-CELSIUS Collaboration [12] is used. For $Q = 15$ MeV, we find $C_1 = (0.001 \pm 0.001)\ \mu b/\mathrm{sr}$ and $C_2 = (-0.002 \pm 0.003)\ \mu b/\mathrm{sr}$. For $Q = 72$ MeV, we obtain the fit parameters $C_1 = (0.104 \pm 0.006)\ \mu b/\mathrm{sr}$ and $C_2 = (0.020 \pm 0.012)\ \mu b/\mathrm{sr}$.

At $Q = 15$ MeV, we find no evidence for partial waves beyond s-wave production. At $Q = 72$ MeV, we find evidence for significant contributions of higher partial waves. If we conclude from the finite coefficient C_1 of the $\sin\theta_\eta$ term that both Ps and Pp give significant contributions, then the vanishing (within errors) coefficient C_2 points to a cancellation between $(Pp)^2$ and Ss^*Sd contributions.

Previously, in the COSY-11 analysis of the 15.5 MeV $M(pp)$ shape, it was suggested that the high-mass region was a signal for a Ps contribution at $Q = 15$ MeV [16]. If this is indeed present in the data, then the small coefficient C_1 would indicate a small Pp contribution at this excess energy. At $Q = 72$ MeV, Petren *et al.* [12] found that a sizable Pp contribution is needed to get the valley along the diagonal of the Dalitz plot for the $pp \to pp\eta$ reaction. Maximal Ss^*Sd interference there was suggested to explain the angular distribution of η production at $Q = 40$ MeV.

Altogether, the previous results and the ones presented in this Letter have the following interpretation.

First, the data indicate just s-wave production at $Q = 15$ MeV. This result contradicts predictions based on single meson exchange, as shown in Fig. 3.

Measurements of the isospin dependence of η meson production in proton-nucleon collisions have revealed that the total cross section for the quasifree $pn \to pn\eta$ exceeds the corresponding cross section for $pp \to pp\eta$ by a factor of about 3 at threshold and by a factor of 6 at higher excess energies between about 25 and 100 MeV [13,18]. This isospin dependence is interpreted as evidence for a strong isovector exchange contribution, which exhibits (partial) cancellation in proton-proton collisions and addition in proton-neutron collisions. This isovector exchange was interpreted in terms of the ρ meson in Ref. [22] and π exchange in Ref. [24]. These one-boson exchange models, when fit to early data on η production, made predictions for A_y, as shown in Fig. 3 with $A_y(\theta_\eta) = \mathcal{A}\sin 2\theta_\eta$, where $|\mathcal{A}| = 0.18$ at $Q = 15$ MeV. Note here that these ρ [22] and π [24] exchange curves come with opposite sign; i.e., the distribution is shifted by $\theta_\eta = 90$ degrees. One possible explanation might be cancellation through destructive interference between π and ρ exchanges in η production in proton-proton collisions very close to threshold, together with a strong (spin-independent) scalar σ exchange contribution.

Cancellation of $(Pp)^2$ and Ss^*Sd interference terms at $Q = 72$ MeV suggests a phase cancellation of various meson exchanges and resonance contributions, e.g., associated with the nucleon resonances $S_{11}(1535)$, $D_{13}(1520)$, and $P_{11}(1440)$.

To summarize, we have measured the spin analyzing power for η production close to threshold with precision improved by 1 order of magnitude. For excess energy $Q = 15$ MeV, the data are consistent with the η production process in the pure s wave. We find evidence of higher partial waves at $Q = 72$ MeV. The Ps^*Pp interference determines the shape of the measured analyzing power with cancellation of Ss^*Sd and $(Pp)^2$ interference terms. The data contradict predictions of presently available meson exchange models of the production mechanism. The analyzing power complements previous measurements of the energy and angular distribution of η meson production and provides new valuable constraints for future model building.

We thank C. Wilkin for helpful communications. This work was supported by the Polish National Science Centre through Grants No. 2013/11/N/ST2/04152, No. 2014/15/N/ST2/03179, and No. 2016/23/B/ST2/00784; the Forschungszentrum Jülich FFE Funding Program of the Jülich Center for Hadron Physics; and the Swedish Research Council.

*Present address: Institut für Kernphysik, Johannes Gutenberg-Universität Mainz, Johann-Joachim-Becher Weg 45, 55128 Mainz, Germany.
†Present address: Peter Grünberg Institut, PGI-6 Elektronische Eigenschaften, Forschungszentrum Jülich, 52425 Jülich, Germany, and Institut für Laser-und Plasmaphysik, Heinrich-Heine Universität Düsseldorf, Universitätsstr. 1, 40225 Düsseldorf, Germany.
‡Present address: Jülich Centre for Neutron Science JCNS, Forschungszentrum Jülich, 52425 Jülich, Germany.
§Present address: Department of Physics, Harvard University, 17 Oxford Street, Cambridge, MA 02138, USA.
‖Present address: INFN, Laboratori Nazionali di Frascati, Via E. Fermi, 40, 00044 Frascati (Roma), Italy.

[1] B. Krusche and C. Wilkin, Prog. Part. Nucl. Phys. **80**, 43 (2015).
[2] P. Moskal, M. Wolke, A. Khoukaz, and W. Oelert, Prog. Part. Nucl. Phys. **49**, 1 (2002).
[3] S. D. Bass and P. Moskal, Acta Phys. Pol. B **47**, 373 (2016).
[4] T. E. O. Ericson and W. Weise, *Pions and Nuclei* (Clarendon Press, Oxford, England, 1988).
[5] C. Hanhart, Phys. Rep. **397**, 155 (2004).
[6] P. Winter *et al.*, Phys. Lett. B **544**, 251 (2002); **553**, 339(E) (2003).
[7] R. Czyzykiewicz *et al.*, Phys. Rev. Lett. **98**, 122003 (2007).
[8] F. Balestra *et al.*, Phys. Rev. C **69**, 064003 (2004).
[9] S. Brauksiepe *et al.*, Nucl. Instrum. Methods Phys. Res., Sect. A **376**, 397 (1996).
[10] H. Calen *et al.*, Phys. Lett. B **366**, 39 (1996).
[11] H. Calen *et al.*, Phys. Rev. Lett. **79**, 2642 (1997).
[12] H. Petrén *et al.*, Phys. Rev. C **82**, 055206 (2010).
[13] H. Calen *et al.*, Phys. Rev. C **58**, 2667 (1998).
[14] J. Smyrski *et al.*, Phys. Lett. B **474**, 182 (2000).
[15] M. Abdel-Bary *et al.* (COSY-TOF Collaboration), Eur. Phys. J. A **16**, 127 (2003).
[16] P. Moskal *et al.*, Phys. Rev. C **69**, 025203 (2004).
[17] P. Moskal *et al.*, Eur. Phys. J. A **43**, 131 (2010).
[18] P. Moskal *et al.*, Phys. Rev. C **79**, 015208 (2009).
[19] E. Chiavassa *et al.*, Phys. Lett. B **322**, 270 (1994).
[20] F. Hibou *et al.*, Phys. Lett. B **438**, 41 (1998).
[21] A. M. Bergdolt *et al.*, Phys. Rev. D **48**, R2969 (1993).
[22] G. Faldt and C. Wilkin, Phys. Scr. **64**, 427 (2001).
[23] K. Nakayama, J. Speth, and T. S. H. Lee, Phys. Rev. C **65**, 045210 (2002).
[24] K. Nakayama, J. Haidenbauer, C. Hanhart, and J. Speth, Phys. Rev. C **68**, 045201 (2003).
[25] M. T. Pena, H. Garcilazo, and D. O. Riska, Nucl. Phys. **A683**, 322 (2001).
[26] A. Deloff, Phys. Rev. C **69**, 035206 (2004).
[27] R. Shyam, Phys. Rev. C **75**, 055201 (2007).
[28] S. D. Bass, Phys. Lett. B **463**, 286 (1999).
[29] R. Maier, Nucl. Instrum. Methods Phys. Res., Sect. A **390**, 1 (1997).
[30] C. Patrignani *et al.* (Particle Data Group), Chin. Phys. C **40**, 100001 (2016).
[31] H. H. Adam *et al.* (WASA-at-COSY Collaboration), arXiv: nucl-ex/0411038.
[32] C. Bargholtz *et al.* (CELSIUS/WASA Collaboration), Nucl. Instrum. Methods Phys. Res., Sect. A **594**, 339 (2008).
[33] P. Adlarson *et al.*, Phys. Rev. C **94**, 065206 (2016).
[34] M. Hodana, P. Moskal, I. Ozerianska, and M. Zieliński (WASA-at-COSY Collaboration), Acta Phys. Pol. B **45**, 697 (2014).
[35] Madison convention, *Proc 3rd International Symposium on Polarization Phenomena in Nuclear Physics, Madison 1970*, edited by H. H. Barschall and W. Haeberli (Univ. of Wisconsin Press, Madison, WS 1971), p. xxv.
[36] I. Schatti-Ozerianska, Ph.D. thesis, Jagiellonian University, 2016.
[37] F. Bauer and K. Busser (EDDA Collaboration), Nucl. Instrum. Methods Phys. Res., Sect. A **431**, 385 (1999).
[38] M. Altmeier *et al.* (EDDA Collaboration), Phys. Rev. Lett. **85**, 1819 (2000).
[39] I. Schatti-Ozerianska, P. Moskal, and M. Zieliński, Acta Phys. Pol. B **46**, 153 (2015).
[40] I. Ozerianska, P. Moskal, and M. Zieliński (WASA-at-COSY Collaboration), EPJ Web Conf. **81**, 02013 (2014).
[41] M. Hodana, P. Moskal, and I. Ozerianska, Acta Phys. Pol. B Proc. Suppl. **6**, 1041 (2013).
[42] H. O. Meyer *et al.*, Phys. Rev. C **63**, 064002 (2001).